IEEE Access
Multidisciplinary | Rapid Review | Open Access Journal

Received May 8, 2021, accepted May 26, 2021, date of publication June 2, 2021, date of current version June 11, 2021.

Digital Object Identifier 10.1109/ACCESS.2021.3085336

Nonlinear Feedback-Based Path Following Control for Underactuated Ships via an Improved Compound Line-of-Sight Guidance

ZUOJING SU AND XIANKU ZHANG
Navigation College, Dalian Maritime University, Liaoning 116026, China
Corresponding author: Xianku Zhang (zhangxk@dlmu.edu.cn)

This work was supported in part by the National Science Foundation of China under Grant 51679024, in part by the Fundamental Research Funds for the Central Universities under Grant 3132020138, and in part by the University 111 Project of China under Grant B08046.

ABSTRACT To promise the high fidelity of path following control for the underactuated ship from the aspect of the nautical practice, this paper develops a nonlinear feedback-based control scheme with an improved compound line-of-sight (ICLOS) guidance law, which has the energy-saving and efficient performance. Based on the methodology of the nonlinear disturbance observer and method of reduced-order extended state observer (ESO), a reduced-order state nonlinear sideslip angle observer is developed for online estimation of the time-varying sideslip angel caused by external disturbances, and a sideslip angle controller is incorporated to avert the sharp acting of actuators. Meanwhile, unlike the traditional line-of-sight (LOS) guidance law, a time-varying lookahead distance is designed as a function that relates to the ship' cruising speed and the cross track error, while the advance steering distance is also variable responding to the ship's length and turning angle, both of them make the turning process smoother. In the control scheme, the second-order closed-loop gain shaping algorithm (CGSA) is employed to design a concise robust controller, where the fuzzy logic system (FLS) is introduced to adjust the integral coefficient online to improve the transient performance. In addition, to further reduce the steering frequency and energy consumption of the system, nonlinear feedback technology (NFT) is adopted. Numerical simulation and comprehensive comparisons are conducted to demonstrate the remarkable performance and superiority of the proposed path following control system.

INDEX TERMS Path following control, closed-loop gain shaping algorithm (CGSA), fuzzy logic system (FLS), nonlinear feedback technique (NFT), improve compound line-of-sight (ICLOS).

I. INTRODUCTION

For a conventional ship, it is common to consider the motion in the surge, sway, and yaw, while it only has propellers and rudder to control the motions. In this configuration, only the surge and yaw degrees of freedom (DOF) are directly controlled, thus the dynamics of the ship are underactuated which increases the difficulty of the ships' motion control [1]. However, with the increasing prosperity of guidance and navigation technology as well as control theory, plenty of higher performance and versatility control schemes for the underactuated ship's motion control are developed [2], [3]. As an important content of ship's motion control research, track keeping control which consists of path following control and trajectory tracking control has also received great attention and development. This paper is mainly focused on the path following control of underactuated ships exposed to wind, waves, and ocean currents, which deals with a design control scheme that drives ships to reach and follow a predefined path without time constraints.

Ship's path following control can be divided into two types: direct path following control and indirect path following control [4], [5]. [6] designed a ship path following controller based on the characteristic model, which is convenient to adjust the controller structure as the navigation environment changes. In [7], a dynamic virtual ship guidance principle was proposed, which used a virtual ship to generate a reference path and then incorporated the neural network and dynamic

The associate editor coordinating the review of this manuscript and approving it for publication was Ning Sun.

surface control technique to track the predefined path. And the backstepping method and the Lyapunov stability theory were popularly employed to realize the path following of underactuated ships [2], [8], [9]. These control schemes are all direct path following control and rely heavily on the mathematical model of the system as well as the design of these controllers is complicated due to the ship's complex nonlinearity and uncertainty characteristics.

Conversely, in the indirect path following control scheme design process, the mathematical models and control methods independent of each other, which makes the design difficulty significantly reduced [10]. It is mainly composed of two parts, guidance subsystem and course keeping control subsystem, where the guidance subsystem is used to generate the desired heading signal based on the acquired path and environment information, and the course keeping control subsystem is used for tracking the desired heading signals generated by the guidance subsystem. Since the indirect path following control is similar to the actual ship maneuvering behavior of the crew, the modular design concept also enables it to directly apply mature guidance technology and course keeping control theory, which has strong practical application value and becomes the commonly used method of path following [11]–[14].

There are many guidance approaches, including Light-of-Sight guidance (LOS), Constant Bearing guidance (CB), Pure Pursuit guidance (PP), Vector Field guidance (VF), and so on, which can be used for designing the guidance subsystem [15]. Because of the low sensitivity to high-frequency noises, fewer design parameter requirements, and low computational burden, the LOS guidance has been widely used in the track keeping controller design compared to others. And the uniform semi-global exponential stability was proved to be achievable for a class of proportional LOS guidance laws used for vehicle path following control [16]. However, the traditional proportional LOS guidance is vulnerable to external disturbance that results in deviation problems, especially in tracking curved paths [17].

To eliminate the constant offsets induced by the constant, or slow time-varying, environmental forces which can be observed as a nonzero sideslip angel, a class of modified LOS guidance was developed. The straightforward solution to solve this problem is to measure the sideslip angle, which is impractical due to the expensive cost and low precision [18]. An alternative approach is to bring an integral term into the traditional LOS guidance to alleviate the effect of sideslip angle, which is originally proposed in [17] and called integral LOS (ILOS) guidance. In [16], an adaptive LOS (ALOS) guidance is proposed where the sideslip angle is treated as an unknown constant parameter and can be identified by an adaptive term online. It should be noted that the sideslip angle in these guidance lows is treated as a constant while it is actually time-varying in the reality. To deal with time-varying sideslip angel, a predictor LOS (PLOS) guidance, as well as a reduced-order extended state observer LOS (ESO-based LOS) guidance for online estimation and identification of the time-varying sideslip angle, are presented in [5], [19]. A bounded gain forgetting adaptive estimator was designed to predict the time-varying sideslip angle and compensate it in [20]. In addition, to improve the tracking effects of LOS guidance, the lookahead distance is designed as a function of the cross track error to improve the LOS guidance law [21], [22]. Nevertheless, these guidance laws may not applicable to practical conditions ''waypoint-based planned route for ships'', where the sideslip angle, lookahead distance, advance steering distance as well as the ship's speed should be overall considered.

For the course keeping control subsystem, in view of the cruising speed of ships is constant on the open sea, the course keeping control becomes a rudder-based yaw control problem. With the prosperity of control theory, various advanced control methods can be used to solve this problem [23]–[26]. In this study, a nonlinear feedback-based controller which has the characteristics of concise form, strong robustness, fewer parameters, and energy saving will be developed.

Since the proportion integration differentiation (PID) control method does not rely on a specific mathematical model and has relatively few control parameters, it has been widely applied to ship course keeping control [27], [28]. However, the adjustment of the parameters is very difficult and often depends on designers' experiences. Thus, the closed-loop gain shaping algorithm (CGSA), which is a strong engineering method and has been widely used in the ship's motion control [29]–[31], is adopted to quickly design a robust PID controller with tuned parameters. Meanwhile, considering the PID controller is too sensitive to high-frequency interference, which is easy to cause frequent operations, and lacks the ability to adapt to ship dynamics and sea conditions. The fuzzy control is introduced to deal with the above-motioned problems. Although its control accuracy is not high, it has the advantages of not relying on mathematical models, insensitive to parameter changes, and strong in robustness. Complementing the advantages of the two methods can achieve good results, and there have been many successful examples [32]–[34].

Furthermore, from the perspective of energy saving and high efficiency, we have further improved the controller by employing the nonlinear feedback technique (NFT). As mentioned above, PID control has easily interfered to cause frequent operations, while fuzzy control is difficult to eliminate static errors, which makes it easy to cause high-frequency oscillation in small error, resulting in frequent operations of ships steering gear to consume a lot of energy. NFT is a technology that can improve the energy efficiency of the system and achieve the same control effect with minor control action under the unchanged control law. In addition, its effectiveness has been validated through the theoretical analysis and the simulation experiments relating to the ship course keeping control [35]–[39].

Motivated by the above observations, this paper investigates both the path following guidance and the rudder-based yaw controller for the underactuated ship. The main contributions of the paper can be summarized as follows.

(1) For the guidance subsystem: Based on ESO-based LOS guidance and with consideration of nautical practice, an improved compound LOS guidance embracing a nonlinear sideslip angle observer, a sideslip angle controller, a lookahead distance adjuster, and an advance steering distance adjuster are proposed, which can enhance both dynamic and static performance.

(2) For the course keeping control subsystem: The second-order CGSA is employed to design a PID controller with a first-order filter, and the FLS and NFT are further introduced to improve transient performance and save energy.

This paper is organized as follows. In Section 2, the preliminaries and problem formulation are presented. The nonlinear feedback-based control law is devised for the ship course keeping in Section 3, and the improved compound LOS guidance law is elucidated with stability analysis in Section 4. The simulation and analysis are carried out in Section 5. Section 6 concludes the entire work.

II. PRELIMINARIES

A. MATHEMATICAL MODEL

As for path following, only three motions (namely surge, sway and yaw) need to be considered. In this study, a 3-DOF model is established to describe the motion of the ship, where the attitudes are described by (1) of the kinematic model [1].

$$\begin{aligned} \dot{x} &= u\cos(\psi) - v\sin(\psi) \\ \dot{y} &= u\sin(\psi) + v\cos(\psi) \\ \dot{\psi} &= r \end{aligned} \tag{1}$$

where x, y, ψ denotes the position the orientation of the ship with respect to the earth-fixed inertial frame; and u, v, r denotes the velocity/angular rate in surge, sway and yaw DOF in the body-fixed frame, respectively.

In consideration of the internal perturbations and external environmental disturbances, the nonlinear Norrbin model is employed as the kinetic model of the ship [40].

$$\dot{\boldsymbol{X}}_{(2)} = \boldsymbol{A}_{(2)}\boldsymbol{X}_{(2)} + \boldsymbol{B}_{(2)}\delta_c + (\boldsymbol{I}'_{(2)})^{-1}[\boldsymbol{F}'_{\text{Non}} + \boldsymbol{F}'_{\text{Wind}} + \boldsymbol{F}'_{\text{Wave}}] \tag{2}$$

where $\boldsymbol{X}_{(2)} = [v\ r]^T$ is the velocity and angular rate of the ship; $\boldsymbol{A}_{(2)}, \boldsymbol{B}_{(2)}$ are dynamic coefficient matrices; δ_c is the control rudder angle; $\boldsymbol{I}'_{(2)}$ is the inertial force derivative matrix; $\boldsymbol{F}'_{\text{Non}}$, $\boldsymbol{F}'_{\text{Wind}}$ and $\boldsymbol{F}'_{\text{Wave}}$ are the nonlinear fluid force, wind force, and wave force term, respectively.

The nonlinear fluid force term $\boldsymbol{F}'_{\text{Non}}$ is formulated as

$$\boldsymbol{F}'_{\text{Non}} = \begin{bmatrix} \boldsymbol{Y}'_{NON} \\ \boldsymbol{N}'_{NON} \end{bmatrix} = \begin{bmatrix} \boldsymbol{f}_Y(\boldsymbol{v}, \boldsymbol{r}) \\ \boldsymbol{C}\boldsymbol{f}_N(\boldsymbol{v}, \boldsymbol{r}) \end{bmatrix} \tag{3}$$

where proportional coefficient $\boldsymbol{C}$ is the dimensionless cross-flow coefficient; $\boldsymbol{f}_Y(\boldsymbol{v}, \boldsymbol{r})$ and $\boldsymbol{f}_N(\boldsymbol{v}, \boldsymbol{r})$ are the function of the nonlinear lateral force and moment which can be consulted in [40] for the details.

The wind force term $\boldsymbol{F}'_{\text{Wind}}$ can be divided into average wind and fluctuating wind. The average wind component is converted into the wind equivalent rudder angle expressed in (4), and the fluctuating wind component is simulated by the white noise [41].

$$\delta_w = K'\left(\frac{V_w}{V_L}\right)\sin\psi_w \tag{4}$$

where V_w, V_L, K' and ψ_w denote wind speed, ship speed, wind coefficient and the wind angle on the bow, respectively.

For the wave force term $\boldsymbol{F}'_{\text{Wave}}$, a linear approximation of International Towing Tank Conference (ITTC) spectral density function $y(s) = h(s)\omega_G(s)$ is used to replace the complex nonlinear wave model. where, $\omega_G(s)$ is a zero-mean Gaussian white noise process with a power spectrum of $G_\omega(\omega) = 1.0$ and $h(s)$ is a second order transfer function. Supposing the wave disturbance directly affects the ship's heading and using the ITTC spectrum, the model of wave disturbance corresponding to Beaufort No.6 is formulated as

$$\psi_H = \frac{0.4198s}{s^2 + 0.3638s + 0.3675}\omega_G \tag{5}$$

where ψ_H, s are high-frequency wave disturbance, Laplace operator, respectively.

The current interference is regarded as a steady current or current with slow time-varying characteristics, which means that it only affects the position and speed of the ship. And the velocities u, v in (1) can be rewritten as

$$\begin{aligned} u &= u_r + V_C\cos(\gamma_c - \psi) \\ v &= v_r + V_C\sin(\gamma_c - \psi) \end{aligned} \tag{6}$$

$$\begin{aligned} \dot{x} &= u_r\cos\psi - v_r\sin\psi + V_c\cos\gamma_c \\ \dot{y} &= u_r\sin\psi + v_r\cos\psi + V_c\sin\gamma_c \end{aligned} \tag{7}$$

where u_r, v_r represent the velocities of the ship relative to the water; ψ is the heading angle of the ship; V_c, γ_c are the velocity and the direction of the current, respectively.

B. PROBLEM FORMULATION

The path following problem deals with the design of a control scheme to drive the ship to reach and follow a predefined path without time constraints. In nautical practice, ships will navigate along the straight route between the various waypoints at an economic speed on the open sea. In addition, the quartermaster will steer the ship in advance according to the turning angle to make the navigation more stable. The geometric representation of the LOS-guided ship path following is shown in Fig.1.

The predefined path which connects the waypoint $(x_k,\ y_k)$ and $(x_{k+1},\ y_{k+1})$ is a straight line. Let θ represent the path variable. For any given θ, the inertial position of the geometric path is denoted by $P_\theta(x_k(\theta), y_k(\theta))$. Define a local reference frame at $P_\theta(x_k(\theta), y_k(\theta))$ and named it the path-tangential reference frame. The path-tangential angle, which represents the orientation of the path relative to the earth-fixed frame, is given by $\alpha_k = \text{atan2}\left(y'_k(\theta), x'_k(\theta)\right)$, where $x'_k(\theta) = \partial x_k / \partial\theta$, and $y'_k(\theta) = \partial y_k / \partial\theta$.

For the ship located at $(x,\ y)$, the along track error x_e and the cross track error y_e can be expressed in the path tangential

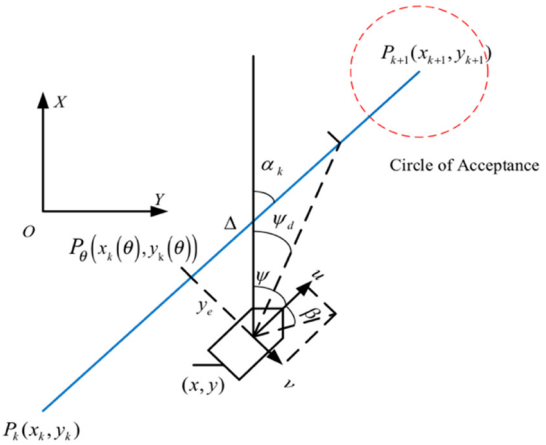

FIGURE 1. Geometric representation of LOS guidance.

reference frame as follow

$$\begin{bmatrix} x_e \\ y_e \end{bmatrix} = \begin{bmatrix} \cos\alpha_k & -\sin\alpha_k \\ \sin\alpha_k & \cos\alpha_k \end{bmatrix}^T \begin{bmatrix} x - x_k(\theta) \\ y - y_k(\theta) \end{bmatrix} \tag{8}$$

Owing to the $P_\theta(x_k(\theta), y_k(\theta))$ is the projection point of the ship's position coordinates (x, y) on the reference path, $x_e = 0$, then the cross track error is formulated as [12]

$$y_e = -\sin\alpha_k (x - x_k(\theta)) + \cos\alpha_k (y - y_k(\theta)) \tag{9}$$

Based on the traditional lookahead based steering method, the guidance heading angle ψ_l can be expressed as (10). And there needs to be a criterion to determine whether to steer to the next tracking path, (11) gives the criteria.

$$\psi_l = \alpha_k + \arctan(\frac{-y_e}{\Delta}) \tag{10}$$

$$(x - x_{k+1})^2 + (y - y_{k+1})^2 \le R^2 \tag{11}$$

where Δ and R denote lookahead distance and the acceptance steering distance, which determine the transient performance of the ship path following control system.

The derivatives of the cross track error are derived by differentiating (9) and combining with (1)

$$\dot{y}_e = U\sin(\arctan\frac{-y_e}{\Delta} - \beta) \tag{12}$$

where $U = \sqrt{u^2 + v^2}$ and $\beta = \arctan(v/u)$ are the resultant and sideslip angle of the ship. In the practical application, the sideslip angle is time-varying and difficult to measure due to environmental disturbances [18].

Based on the above-mentioned analysis, the control objective of this paper is to develop a guidance law, with consideration of time-varying sideslip angle, lookahead distance, and advance steering distance, to guide the ship to track the given path under the wind, wave, and current disturbance, and design a robust and energy-saving course keeping controller to obtain the desired heading angle responding to the guidance. The design objective can be formalized as

$$\lim_{x\to\infty} y_e \le \varepsilon_1, \quad \lim_{x\to\infty} (\psi - \psi_d) \le \varepsilon_2 \tag{13}$$

where ε_1 and ε_2 are very small positive numbers, ψ_d is the desired heading angle.

III. IMPROVED COMPOUND LOS GUIDANCE LAW DESIGN

On account of the sideslip angle is mainly caused by environmental disturbances, which can be time-varying and cause a static track error. Based on the methodology of the nonlinear disturbance observer and method of reduced-order extended state observer originally proposed in [16], a nonlinear sideslip angle observer is designed. Meanwhile, considering the influence of constant lookahead distance and advance steering distance on the transient performance of the path following system, further improvements are made to obtain an improved compound LOS (ICLOS) guidance law in this section.

A. NONLINEAR SIDESLIP ANGLE OBSERVER DESIGN AND ANALYSIS

Taking account that the sideslip angle β is generally small, no more than 5 degrees [42]. This means it is reasonable to approximate $\sin\beta \approx \beta$ and $\cos\beta \approx 1$. Expanding (12), one can get that

$$\dot{y}_e = U\sin(\psi - \alpha_k) + U\cos(\psi - \alpha_k)\beta \tag{14}$$

Define $g = U\cos(\psi - \alpha_k)\beta$. Therefore, as long as the g can be estimated, the estimate of β can be obtained, that is

$$\hat{\beta} = \frac{\hat{g}}{U\cos(\psi_d - \alpha_k)} \tag{15}$$

where $\hat{g}$, $\hat{\beta}$ denote the estimate of g and β, respectively.

To move on, the following assumptions are required.

Assumption 1: There exits an upper bound of $|\dot{g}|$, satisfying $|\dot{g}| < |\dot{g}|_{\mathrm{m}}$.

Assumption 2: The ship's course can track the desired heading angle ψ_d well [14], [43].

Define the estimation error of the sideslip angle $\tilde{g} = g - \hat{g}$, k is the observer gain, and a linear observer is designed as

$$\dot{\tilde{g}} = k(g - \hat{g}) = -k\hat{g} + k(\dot{y}_e - U\sin(\psi_d - \alpha_k)) \tag{16}$$

Since the linear observer requires a known derivative of the track error, which is difficult to obtain in practice, a nonlinear observer contains an auxiliary variable p is constructed as

$$\begin{aligned} \hat{g} &= p + ky_e \\ \dot{p} &= -kp - k(U\sin(\psi_d - \alpha_k) + ky_e) \end{aligned} \tag{17}$$

Differentiating $\hat{g}$ and invoking (16) and (17), it renders

$$\begin{aligned} \dot{\hat{g}} &= \dot{p} + k\dot{y}_e \\ &= kg - k(p + ky_e) \\ &= k\tilde{g} \end{aligned} \tag{18}$$

Then, with the consideration of sideslip angle, the desired heading angle in (14) can be rewritten as follows

$$\psi_d = \alpha_k + \arctan(\frac{-y_e}{\Delta} - \hat{\beta}) \tag{19}$$

Noting that

$$\sin\left(\tan^{-1}\left(\frac{-y_e}{\Delta}-\hat{\beta}\right)\right)=\frac{\frac{-y_e}{\Delta}-\hat{\beta}}{\sqrt{\Delta^2+\left(y_e+\Delta\hat{\beta}\right)^2}}$$
$$\cos\left(\tan^{-1}\left(\frac{-y_e}{\Delta}-\hat{\beta}\right)\right)=\frac{\Delta}{\sqrt{\Delta^2+\left(y_e+\Delta\hat{\beta}\right)^2}} \quad (20)$$

Based on the assumption 2, substitute (20) into (14) gives

$$\dot{y}_e=-\frac{Uy_e}{\sqrt{\Delta^2+\left(y_e+\Delta\hat{\beta}\right)^2}}-\tilde{g}=-k_1y_e-\tilde{g} \quad (21)$$

where, $k_1=\frac{U}{\sqrt{\Delta^2+\left(y_e+\Delta\hat{\beta}\right)^2}}$.

For the subsystem (18), defining a candidate Lyapunov function $V_1=\frac{1}{2}\tilde{g}^2$ and taking the time derivative of V_1 satisfies

$$\begin{aligned}\dot{V}_1&=\tilde{g}(\dot{g}-\dot{\hat{g}})\\&=-k\tilde{g}^2+\tilde{g}\dot{g}\end{aligned} \quad (22)$$

Using Young's inequality, there exist $\tilde{g}\dot{g}\le a_1\tilde{g}^2+\frac{|\dot{g}|_{\mathrm{m}}^2}{4a_1}$ and (22) can be rewrite as

$$\dot{V}_1\le-(k-a_1)\tilde{g}^2+\frac{|\dot{g}|_{\mathrm{m}}^2}{4a_1} \quad (23)$$

Considering the entire error system, define the candidate Lyapunov function $V_2=V_1+\frac{1}{2}y_e^2$ and take time derivative along V_2 with (21) and (23), it yields

$$\dot{V}_2\le-(k-a_1)\tilde{g}^2+\frac{|\dot{g}|_{\mathrm{m}}^2}{4a_1}-k_1y_e^2-y_e\tilde{g} \quad (24)$$

Using Young's inequality, there exist $-\tilde{g}y_e\le a_2\tilde{g}^2+\frac{y_e^2}{4a_2}$. Invoking (24), it renders

$$\dot{V}_2\le-(k-a_1-a_2)\tilde{g}^2-(k_1-\frac{1}{4a_2})y_e^2+\frac{|\dot{g}|_{\mathrm{m}}^2}{4a_1} \quad (25)$$

Then there is $\dot{V}_2\le-\mu V_2+d$.
where, $d=\frac{|\dot{g}|_{\mathrm{m}}^2}{4a_1}\mu=2\min\left\{(k-a_1-a_2),(k_1-\frac{1}{4a_2})\right\}>0$.
Such that, we have

$$0\le V_2\le\frac{d}{\mu}+(V_2(0)-\frac{d}{\mu})e^{-\mu t} \quad (26)$$

The above analysis results show that all error signals are ultimately bounded, and by selecting appropriate design parameters, the ship will track the desired path with arbitrarily small sideslip angle estimation error and track error.

B. ESTIMATED SIDESLIP ANGLE CONTROLLER

Since $\hat{g}=p+ky_e$, while the ship starts steering to the next tracking path, the sudden increase in cross track error will cause the increase of the nonlinear observer output $\hat{g}$. This will cause the desired heading angle ψ_d in (19) to change instantaneously, which will not only cause the saturation of the actuator, but also a large flare of the ship. For these reasons, an estimated sideslip angle controller $\hat{\beta}(t)$ is introduced to the system to avoid this situation.

$$\hat{\beta}(t)=\begin{cases}\beta_0 & \left|\hat{g}(t)-\hat{g}(t-1)\right|>0.01h\\ \dfrac{\hat{g}}{U\cos(\psi-\alpha_k)} & \left|\hat{g}(t)-\hat{g}(t-1)\right|\le0.01h\end{cases} \quad (27)$$

where β_0 is the previous estimated sideslip angle before time t; h is the sampling period; $\hat{g}(t)$ and $\hat{g}(t-1)$ are the estimated values of g at the current and previous sample time respectively.

According to the control mechanism of this controller, when the output $\hat{g}$ changes significantly correspond to the transient process, the observer's auxiliary state p will be updated according to (17) with $\hat{\beta}$ not be updated and kept the previous value β_0. On the contrary, the $\hat{\beta}$ will be updated when the change rate of the $\hat{g}$ is small.

C. LOOKAHEAD DISTANCE ADJUSTER

The velocity path relative angle $\psi_{\mathrm{r}}(y_e)=\arctan(\frac{-y_e}{\Delta})$ can be regarded as a saturation control law that the lookahead distance is the proportional gain. Excessive lookahead distance will result in too slow tracking speed, while too small lookahead distance will increase system overshoot. Meanwhile, when the cross track error is relatively large, a small lookahead distance should be selected without regard to the ship's speed. Accordingly, the lookahead distance should be increased in connection to the ship's speed when the cross track error decreases. Based on the above guidelines, the lookahead distance should be a time-varying parameter with consideration of the cross track error. Whereas, in the traditional LOS guidance law, the lookahead distance is set to 2-5 times the length of the ship. To improve the transient performance of the control system, a time-varying lookahead distance adjuster is employed [12].

$$\Delta(y_e)=(K_1U-\Delta_{\min})e^{-k_2y_e^2}+\Delta_{\min} \quad (28)$$

where K_1, K_2 are controller parameters greater than zero; $\Delta_{\min}$ is minimum lookahead distance when the speed factor is not included.

D. ADVANCE STEERING DISTANCE ADJUSTER

In practice, the seafarer will manipulate the ship in advance according to the steering angle before approaching a certain distance to the waypoint, to avoid the ship's heeling caused by the rapid and large-angle steering. However, in the traditional LOS guidance law, the advance steering distance usually takes a fixed value, 2.2 times the length of the ship, which causes the ship to overshoot at the waypoint and deviate from the track path. Based on numerous simulation experiments, an advance steering distance adjustment strategy, which relates to the turning angle and ship's length, is proposed to improve the performance of the guidance law.

$$L_{turn}=(3\psi_{turn}+1.5)L_{pp} \quad (29)$$

where L_{turn}, ψ_{turn} and L_{pp} are advance steering distance, turning angle and ship's length, respectively.

IV. COURSE KEEPING CONTROLLER DESIGN

In this section, a nonlinear feedback-based concise robust controller, based on CGSA, FLS, and NFT, is designed for the rudder control.

A. LINEAR PID CONTROLLER DESIGN

The CGSA is a simplified H_∞ mixed sensitivity algorithm by directly shaping the singular value curves of $S(s)$ (the sensitivity function) and $T(s)$ (the complementary sensitivity function), and there exists the correlativity $T(s) = I - S(s)$. The complementary sensitivity function $T(s)$ of a typical control system has a lowpass characteristics to guarantee the robust performance, and the largest singular value equals to unit one to follow the reference signal without the tracking error [29]. The high-frequency asymptote slop of $T(s)$ determines how much the system is sensitive to the invalid disturbance frequency and is usually suggested to be 20 dB/dec, 40 dB/dec, and 60 dB/dec. That generates the common shaping selection $T(s) = 1/(T_0 s + 1)^i$, $i = 1; 2; 3$ respectively, which are corresponding to the 1st, 2nd and 3rd order CGSA. (29) presents the formulation of the CGSA.

$$T(s) = \frac{1}{(T_0 s + 1)^i} = \frac{GK}{1 + GK} \tag{30}$$

where the $G(s)$ is the stable control plant, $K(s)$ is the controller, T_0 is the tuning parameter, and the inverse $1/T_0$ is just the frequency bandwidth of $T(s)$.

Consider the course keeping problem for the ships, the responsive nonlinear ship motion mathematical model is selected as the controlled plant G:

$$\ddot{\psi} + \frac{K_0}{T_0}\left(\alpha_1 \dot{\psi} + \beta_1 \dot{\psi}^3\right) = \frac{K_0}{T_0}\delta \tag{31}$$

where ψ is the heading angle, δ is the rudder angle, K_0, T_0 are ship's manoeuvrability indices α_1, β_1 are nonlinear parameters. If the nonlinear term in the equation is ignored, the transfer function model for controller design can be expressed as Nomoto model: $G_{\psi\delta} = K_0/s(T_0 s + 1)$.

Set the bandwidth frequency of the closed-loop system to $1/T_1$ (crossover frequency in the strict sense), let the high frequency asymptote slope be -40dB/dec and $i = 2$, we can obtain the (32).

$$\frac{1}{(T_1 s + 1)^2} = \frac{G_{\psi\delta} K}{1 + G_{\psi\delta} K}, \quad K = \frac{1}{2G_{\psi\delta} T_1 s(\frac{T_1}{2} + 1)} \tag{32}$$

Substitute the Nomoto model into the (31), a typical robust proportional-differential (PD) controller in series with a first-order filter is derived.

$$K(s) = (\frac{1}{K_0 T_1} + \frac{T_0}{K_0 T_1} s)\frac{1}{T_1 s + 2} \tag{33}$$

To eliminate the static error cause by the input interference, an integral term is introduced to (33), that is, a very small constant ε is added to the denominator of the Nomoto model. Then the modified Nomoto model is rewritten as $G_{\psi\delta} = K_0/(T_0 s^2 + s + \varepsilon)$. Substitute it into (33), there is

$$K(s) = (\frac{1}{K_0 T_1} + \frac{T_0}{K_0 T_1} s + \frac{\varepsilon}{K_0 T s})\frac{1}{T_1 s + 2} \tag{34}$$

Furthermore, to adjust the rise time of the system with large inertia, a constant ρ is added at the proportion term of (34) based on the experience of [29]. The controller is updated to (35).

$$K(s) = (\frac{1}{K_0 T_1} + \rho + \frac{T_0}{K_0 T_1} s + \frac{\varepsilon}{K_0 T_1 s})\frac{1}{T_1 s + 2} \tag{35}$$

B. FUZZY LOGIC-BASED PID CONTROLLER DESIGN

The FLS mainly comprises three basic procedures: fuzzification, fuzzy inference, and defuzzification [33]. Firstly, the fuzzification converts the accurate input variables into input grades named as fuzzy variables. Secondly, referring to the fuzzy rule base, the fuzzy inference is conducted and generates fuzzy results. The fuzzy rule base can be constructed according to expertise or online news, which is organized by fuzzy rules. Finally, the defuzzification converts fuzzy variables to accurate output variables.

To benefit from the merits of the CGSA, one can quickly design a concise robust controller with tuned parameters for the system. However, taking into account that the designed integral coefficient ε in (35) whose value is so large as to cause oscillation or overshoot, and too small to completely eliminate the static error. The FLS is employed to approximate the integral coefficient K_i in the designed PID based on CGSA. The input and output values are set to $[-6, +6]$, during the quantization factor of output is set to 0.01, and the triangular membership function is employed. The fuzzy rules include: 1) Reducing the integral coefficient while the control error and its changing rate are large; 2) Increasing the integral coefficient while the control error and its changing rate are small. The fuzzy rules are shown in Fig. 2. Thus, the fuzzy rules applied to adjust the integral coefficient can be express as

$$K_i = \varepsilon_{fuzzy}/K_0 T_1 \tag{36}$$

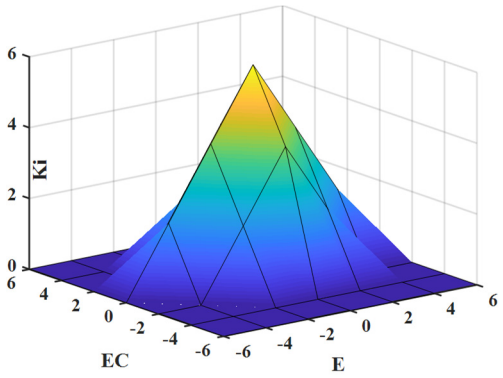

FIGURE 2. Fuzzy rules of the FLS.

C. NONLINEAR FEEDBACK CONTROLLER DESIGN

The NFT is a novel technique used to improve the control performance by employing a nonlinear driven function of error, between the reference signal and the actual system output, as the input of the control law, which can achieve the same control effect with minor control action under the unchanged control law [35]–[39]. However, the researcher should make prudent use of the NFT when the feedback error is too large, which may cause the instability of the control system [37]. The nonlinear feedback system configuration is shown in Fig. 3.

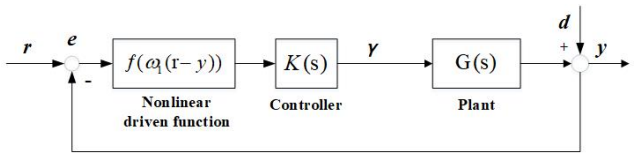

FIGURE 3. Configuration of the nonlinear feedback system.

The nonlinear driven function $f\ (\omega_1\ (r-y))$ is introduced into the scheme instead of the traditional feedback error $(r-y)$, where ω_1 is the dimensionless system frequency; K is the controller to be designed; G is the control plant. Compared to the traditional approach $\gamma = K\,(r-y)$, under the NFT $\gamma = Kf\omega_1\,(r-y)$ which changes the feedback error e from linear to nonlinear by the nonlinear driven function f and the control performance change accordingly. In this paper, the bipolar sigmoid function $f = \left(1-\exp^{-\mu e}\right)/\left(1+\exp^{-\mu e}\right)$ is employed in view of its good performance in ship course keeping control [38], [44]. The experimental results show that the nonlinear feedback driven by the bipolar sigmoid function can obtain good performance on the steady state, dynamic performance, and control output, which could result in the energy-saving, of the closed loop system on the basis of the unchanged controller K.

V. SIMULATION STUDY AND ANALYSIS

The indirect path following control system is mainly composed of two parts, namely the guidance subsystem and the course keeping control subsystem. Fig. 4 illustrates the structure of the proposed indirect path following control system. The guidance subsystem, where an ICLOS guidance law is employed, provides desired heading ψ_d for the course keeping control subsystem. And the designed heading controller, where CGSA, FLS and NFT are used to improve the static and dynamic performance of the control system, outputs the command rudder according to the guidance signal and feedback information to steer the ship to track the desired path.

A. COURSE KEEPING CONTROL SIMULATIONS

In this section, simulation results are presented to verify the effectiveness and superiority of the proposed nonlinear feedback-based concise robust controller. As shown in Fig. 4, the course keeping controller is mainly composed of three

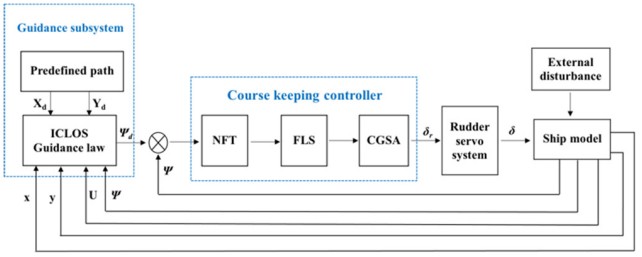

FIGURE 4. Schematic diagram of proposed indirect path following control system.

modules, and its function and technical advantages have been discussed in the previous section. To show more clearly the role of the integrator in eliminating static errors and the FLS in suppressing oscillation or overshoot, a robust PD controller (equation (33)) and fuzzy controller are selected to compare with the proposed controller in the course keeping control experiments. The simulation plant of interest is a multipurpose training ship "YUPENG", her mainly particulars in full load condition are demonstrated in Table 1. Based on these parameters, the parameters for the nonlinear Nomoto model are calculated as $K_0 = 0.38\text{s}^{-1}$, $T_0 = 297.75\text{s}$, $\alpha = 11.95$, $\beta = 23928.91$.

TABLE 1. Particulars of training ship YUPENG.

Particulars	Values	Particulars	Values
L[m]	189	V[kn]	17.3
B[m]	27.8	∇[m^3]	42293.0
X_C[m]	-1.8	d_M[m]	11.0
A_R[m^2]	38	C_b[m]	0.72

In the experiments, the parameters in the linear robust controller and nonlinear driven function are as follows: $T_1 = 3\text{s}$, $\rho = 6$, $\mu = 0.5$. And a rudder servo system is also considered in the simulation, steering engine is modeled as a system with single hydraulic circuit analog control variable, the maximum rudder rate is $\pm 5°/\text{s}$ and the saturation rudder angle is $\pm 35°$. The wind scale is Beaufort NO.6 and the wind angel on the bow is 50°, the equivalent rudder angle of wind is $\delta_w = 3°$, and the equivalent wave interference is expressed as (4). With the initial heading 000°, the desired heading 070°, and the simulation time 600s. One can get the comparison results under two different controllers, which are shown in Fig. 5.

It is noted that there is a static error induced by the interference in the Fig. 5(a) and frequent large rudder angle control in Fig. 5(b) in the fuzzy and robust PD control process, respectively. Which means it is difficult to accurately control the ship's heading to follow the desired heading, and more energy consumption with the wear and tear of the steering gear. What's more, it will generate the rolling of the ship and affect the safety of navigation in the heavy sea condition. On the contrary, since the integrator in the proposed

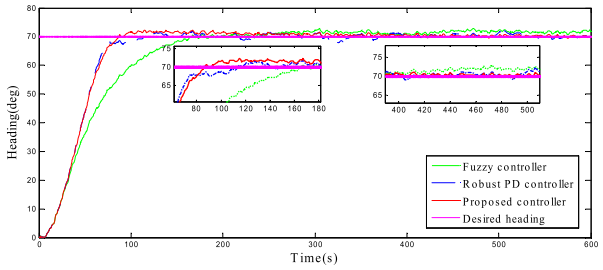

(a)

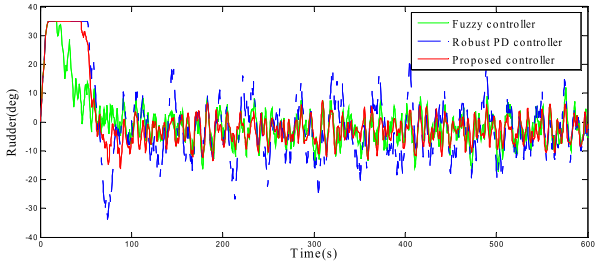

(b)

FIGURE 5. Comparison of the control effects: Fuzzy controller (green dashed line), Robust PD controller (blue dot-dash line) and Proposed controller (red solid line). (a) Heading control. (b) Rudder control.

controller, the static error is eliminated well. However, the proposed controller enables the ship to track the desired heading with a small deviation, while it also causes an overshoot. In benefit from the introduced FLS, the maximum overshoot is about 2° and there is no overshoot in the fuzzy control process. Moreover, thanks to the application of NFT, the steering frequency and amplitude are greatly reduced compared with the other two controllers which shown in Fig. 5(b).

Furthermore, to better compare the three control schemes, mean absolute error (MAE), mean control input (MCI) and mean total variation (MTV), which are formulated in (37), are introduced to quantitative the performance of the controllers in course keeping and energy consumption. MAE is used to measure the performance of the system response, MCI and MTV measure properties of energy consumption and smoothness, respectively. Table 2 gives the quantitative results of the three controllers.

$$\begin{aligned} \mathrm{MAE} &= \frac{1}{t_\infty - t_0}\int_{t_0}^{t_\infty} |\psi_r - \psi(t)|dt \\ \mathrm{MCI} &= \frac{1}{t_\infty - t_0}\int_{t_0}^{t_\infty} |\delta(t)|dt \\ \mathrm{MTV} &= \frac{1}{t_\infty - t_0}\int_{t_0}^{t_\infty} |\delta(t) - \delta(t-1)|dt \end{aligned} \tag{37}$$

From the data point of view, the specific gaps in the performance of the controllers can be observed more intuitively. Consistent with the above analysis, the proposed controller has the shortest settling time t_s and smallest value of MAE, which means it is good at anti-interference. In addition, compared with fuzzy control and robust PD control, the MCI value of the proposed controller is reduced by 12% and 42% respectively, which indicates the average rudder angle

TABLE 2. Quantitative comparison of the controllers.

Control scheme	t_s	MAE	MCI	MTV
Fuzzy controller	166s	0.1334	0.1178	0.0855
Robust PD controller	117s	0.0986	0.1781	0.1320
The proposed controller	88s	0.0973	0.1034	0.0686

applied is small. Meanwhile, the MTV value of the proposed is reduced by 19% and 48% than the other two controllers, respectively, which implies the steering frequency is significantly reduced. From the data analysis, one can find that through the NFT, the overall performance of the system has been greatly improved. Compared with the other two controllers, it has certain advantages in energy efficiency and protection of the actuator.

B. PATH FOLLOWING CONTROL SIMULATIONS

1) EFFECTIVENESS ANALYSIS OF THE ICLOS

Firstly, a straight path connecting two waypoints is adopted to test the tracking ability of the proposed guidance law. Meanwhile, to demonstrate the impact of NFT on the entire control system and its effect on improving energy efficiency, the proposed path following control scheme (hereinafter referred to as ICLOS) with and without NFT are tested for straight path tracking comparison analysis in this section. The coordinates of the two waypoints in the geodetic coordinate system are (0, 0) and (6000, 6000), respectively. The initial position of the subject ship is (−200, 100), and the initial heading angle is 000°. The longitudinal velocity u of the ship is 17.3 knot (the cruising speed), and the lateral velocity is set to 0.0001 m/s. The wind and wave interference remains unchanged. The current velocity is 2 knots and its direction is due east. The course keeping control subsystem remains unchanged. Fig. 6 shows the path following effect, track error, estimated and actual sideslip angle, rudder angle of the path following control system.

The Fig. 6(a) demonstrates that the CILOS can track the desired path at a faster speed and maintain a small static error with it. And the partial enlarged view of Fig. 6(a) shows the NFT does not have much influence on the overall track keeping control effect that the desired path can be tracked well with or without NFT. However, Fig. 6(d) illustrates that, without affecting the control effect, the steering frequency and amplitude of the rudder have been improved to a certain extent under the employment of NFT. As in the previous analysis, the energy efficiency of the control system can be improved by the NFT without the change of the control law. Fig. 6(b) presents the variation of the track error. As the ship approaches the desired path and steadily maintains the desired heading along the straight path, the track error gradually decreases and remains within a small error, which is also consistent with the results in the Fig. 6(a). Since the sideslip angle observer is the key to obtain the desired heading angle

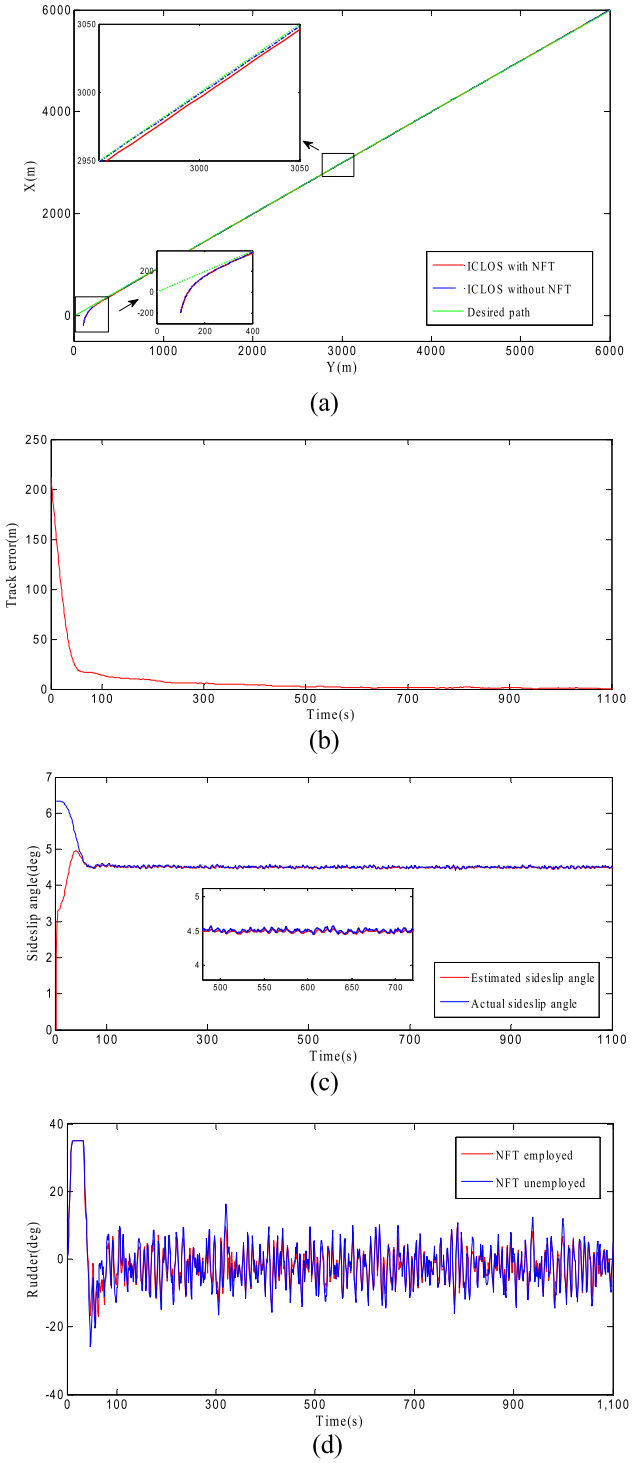

FIGURE 6. Straight path tracking results of the ICLOS. (a) Path following effect. (b) Track error. (c) Estimated and actual sideslip angle. (d) Rudder angle.

in the ICLOS, its accuracy and convergence speed are the performances that need to be paid attention to. It can be seen from the Fig. 6(c) that at the initial moment, as the heading of the ship changes continuously, the sideslip angle is also constantly changing, but the estimated sideslip angle has been converging towards the actual value at a fast speed until it finally maintained at 4.6 degrees which caused by the external disturbance. Therefore, it can be said that, under the combined effect of the ICLOS guidance subsystem and the nonlinear feedback-based control subsystem, the proposed path following control system has a good path following capability in the straight path tracking scenario.

2) COMPARISON ANALYSIS FOR DOG-LEG PATH FOLLOWING

In this section, the comparison simulations of dog-leg path following are conducted to demonstrate the superiority of the ICLOS. To better demonstrate the improvement of the guidance performance with the sideslip angle controller, the lookahead distance adjuster and the advance steering distance adjuster, the ICLOS is compared with an improved variable radius LOS path following control scheme with a nonlinear fuzzy course keeping controller (hereinafter referred to as FLOS) which proposed in [32].

According to [32], seven waypoints which presented in the Table 3, are selected for verifying the effect of the track keeping control schemes. In consideration of the strong coupling to sway and yaw motion during the dog-leg path tracking process of the ship, especially the rapid change of the lateral speed during the turning process which will cause a drastic change in the sideslip angle, as well as to be consistent with [32] and actual nautical situations, the nonlinear Norrbin model expressed in (2) is adopted in this section.

TABLE 3. Simulation waypoints [32].

Waypoint	X(m)	Y(m)
WP-1	0	0
WP-2	1846.2	461.4
WP-3	2769	4615.5
WP-4	-2769	8769
WP-5	-2769	13846.2
WP-6	1846.2	18000
WP-7	0	8307.6

It can be seen from Fig. 7(a) that both control schemes can track the straight path section of the dog-leg path very well. However, benefited from the design of time-varying lookahead distance and advance steering distance, the ICLOS has a smoother trajectory at the waypoints, while the FLOS has an overshoot distance. In particular, using the FLOS, a serious deviation which more than 400 m with a sharp turn occurred at the WP-2 and WP-6, which is extremely unfavorable in nautical practices. The Fig. 7(b) shows the track error change of the subject ship during the path tracking process. Although the ICLOS will generate a large track error at the waypoints which showed in Fig. 7(b), the turning angle is small, and the ship is not prone to serious heeling, which

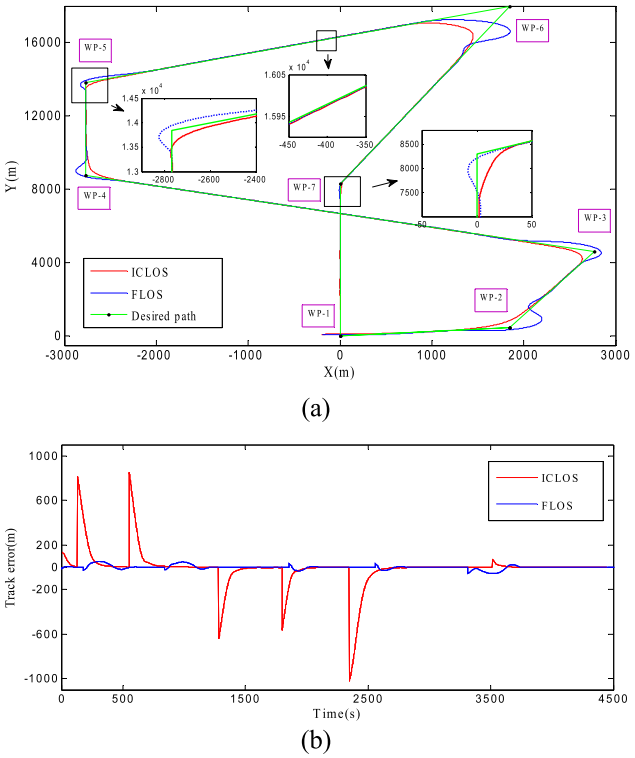

FIGURE 7. Comparison of the dog-leg path tracking results: ICLOS (red solid line) and FLOS (blue dashed line).

not only meets the requirements of navigational safety, but conforms to the practice of navigation. And due to the FLOS makes the subject ship travel close to the desired path, its track error is very small. Nonetheless, as shown in Fig. 7(a), it is easy to cause sharp turning and large overshoot distance at the turning point which is neither safe nor in line with nautical practices.

Furthermore, from the tracking situation of the sideslip angle shown in Fig. 8, one can have a deeper understanding of the advantages of the nonlinear sideslip angle observer designed in this paper. From a global perspective, the observer can estimate and track the sideslip angle very well, and also enable the guidance subsystem to provide accurate desired heading to the course keeping control subsystem

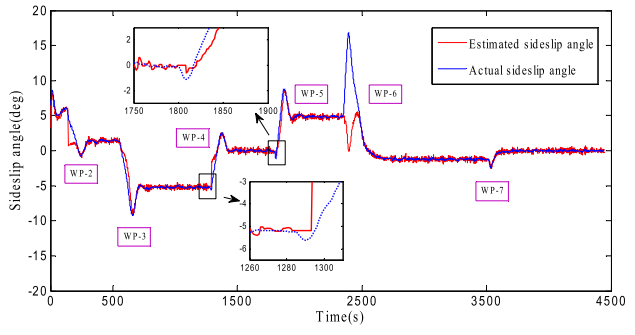

FIGURE 8. Sideslip angle observer outputs of the ICLOS.

for heading control, to realize the purpose of path following. Meanwhile, notice that the estimated sideslip angle not only does not track the actual sideslip angle, but the value is reversed at the WP-6. This is related to the mechanism of the controller designed in this paper, which presented in (27), and is also related to the steering angle at that point being close to the reverse direction. The enlarged diagram in Fig. 8 also shows that, when the sideslip angle changes rapidly, the estimated value unchanged by the mechanism of the controller, which avoids the actuator saturation and frequent operation. Therefore, the estimated sideslip angle does not change when a large steering angle is conducted at the WP-6, but as the heading changes steadily and gradually changes in the opposite direction, the estimated value starts to tracks towards the opposite value.

VI. CONCLUSION

Based on the indirect path following control design ideas and nautical practice, a nonlinear feedback-based path following control system is developed in this paper. This system consists of two subsystems: 1) Guidance subsystem. Based on the ESO-based LOS guidance, an improved version is developed to for online estimation of the time-varying sideslip angel, with a sideslip angle controller incorporated to avert the sharp acting of actuators. In addition, a time-varying lookahead distance and advance steering distance is designed to improve the turning process and consistent with the nautical practice. 2) Course keeping control subsystem. A nonlinear feedback-based robust and energy-efficient controller is proposed which absorbs the advantages of CGSA, FLS and NFT. Meanwhile, simulation results validate the effectiveness and robustness of the proposed path following control system with external disturbances and show its superiority in path tracking and energy saving.

ACKNOWLEDGMENT

Much appreciations to each reviewer for their valuable comments and suggestions to improve the quality of this article.

REFERENCES

[1] T. I. Fossen, *Handbook of Marine Craft Hydrodynamics and Motion Control*. New York, NY, USA: Wiley, 2011.
[2] G. Zhang and X. Zhang, "Concise robust adaptive path-following control of underactuated ships using DSC and MLP," *IEEE J. Ocean. Eng.*, vol. 39, no. 4, p. 39, 685-694, Nov. 2013.
[3] H. Chen and N. Sun, "Nonlinear control of underactuated systems subject to both actuated and unactuated state constraints with experimental verification," *IEEE Trans. Ind. Electron.*, vol. 67, no. 9, pp. 7702–7714, Sep. 2020.
[4] T. I. Fossen and A. M. Lekkas, "Direct and indirect adaptive integral line-of-sight path-following controllers for marine craft exposed to ocean currents," *Int. J. Adapt. Control Signal Process.*, vol. 31, no. 4, pp. 445–463, Apr. 2017.
[5] L. Liu, D. Wang, and Z. Peng, "ESO-based line-of-sight guidance law for path following of underactuated marine surface vehicles with exact sideslip compensation," *IEEE J. Ocean. Eng.*, vol. 42, no. 2, pp. 477–487, Apr. 2017.
[6] Y. Wen, W. Tao, M. Zhu, J. Zhou, and C. Xiao, "Characteristic model-based path following controller design for the unmanned surface vessel," *Appl. Ocean Res.*, vol. 101, Aug. 2020, Art. no. 102293.

[7] G. Zhang and X. Zhang, "A novel DVS guidance principle and robust adaptive path-following control for underactuated ships using low frequency gain-learning," *ISA Trans.*, vol. 56, pp. 75–85, May 2015.
[8] K. D. Do, "Global robust adaptive path-tracking control of underactuated ships under stochastic disturbances," *Ocean Eng.*, vol. 111, pp. 267–278, Jan. 2016.
[9] X. Liang, X. Qu, L. Wan, and Q. Ma, "Three-dimensional path following of an underactuated AUV based on fuzzy backstepping sliding mode control," *Int. J. Fuzzy Syst.*, vol. 20, no. 2, pp. 640–649, Feb. 2018.
[10] A. M. Lekkas and T. I. Fossen, "Line-of-sight guidance for path following of marine vehicles," in *Advanced in Marine Robotics*, O. Gal, Ed. LAP LAMBERT Academic Publishing, 2013, ch. 5, pp. 63–92.
[11] B. Min and X. Zhang, "Concise robust fuzzy nonlinear feedback track keeping control for ships using multi-technique improved LOS guidance," *Ocean Eng.*, vol. 224, Mar. 2021, Art. no. 108734.
[12] L. Wan, Y. Su, H. Zhang, B. Shi, and M. S. AbouOmar, "An improved integral light-of-sight guidance law for path following of unmanned surface vehicles," *Ocean Eng.*, vol. 205, Jun. 2020, Art. no. 107302.
[13] J. Miao, S. Wang, M. M. Tomovic, and Z. Zhao, "Compound line-of-sight nonlinear path following control of underactuated marine vehicles exposed to wind, waves, and ocean currents," *Nonlinear Dyn.*, vol. 89, no. 4, pp. 2441–2459, Jun. 2017.
[14] A. M. Lekkas and T. I. Fossen, "Integral LOS path following for curved paths based on a monotone cubic Hermite spline parametrization," *IEEE Trans. Control Syst. Technol.*, vol. 22, no. 6, pp. 2287–2301, Nov. 2014.
[15] M. Breivik and T. I. Fossen, "Guidance laws for autonomous underwater vehicles," *Underwater Vehicles*, vol. 4, pp. 51–76, Jan. 2009.
[16] T. I. Fossen and K. Y. Pettersen, "On uniform semiglobal exponential stability (USGES) of proportional line-of-sight guidance laws," *Automatica*, vol. 50, no. 11, pp. 2912–2917, Nov. 2014.
[17] E. Borhaug, A. Pavlov, and K. Y. Pettersen, "Integral LOS control for path following of underactuated marine surface vessels in the presence of constant ocean currents," in *Proc. 47th IEEE Conf. Decis. Control*, Dec. 2008, pp. 4984–4991.
[18] A. Hac and M. D. Simpson, "Estimation of vehicle sideslip angle and yaw rate," *SAE Trans.*, vol. 109, pp. 1032–1038, Jan. 2000.
[19] L. Liu, "Path following and cooperative control of underactuated unmanned surface vehicles," Ph.D. dissertation, Dept. Marine Eng., Dalian Maritime Univ., Dalian, China, 2018.
[20] Y. Wang, H. Tong, and M. Fu, "Line-of-sight guidance law for path following of amphibious hovercrafts with big and time-varying sideslip compensation," *Ocean Eng.*, vol. 172, pp. 531–540, Jan. 2019.
[21] A. M. Lekkas and T. I. Fossen, "A time-varying lookahead distance guidance law for path following," in *Proc. 9th IFAC Conf. Manoeuvring Control Mar. Craft*, Arenzano, Italy, 2012, pp. 398–403.
[22] X. Chen, Z. Liu, J. Zhang, J. Dong, and D. Zhou, "Path following of underactuated USV based on modified integral line-of-sight guidance strategies," *J. Beijing Univ. Aeronaut. Astronaut.*, vol. 44, no. 3, pp. 489–499, Mar. 2018.
[23] M. M. Islam, S. A. Siffat, I. Ahmad, and M. Liaquat, "Robust integral backstepping and terminal synergetic control of course keeping for ships," *Ocean Eng.*, vol. 221, Feb. 2021, Art. no. 108532.
[24] X.-K. Zhang, Q. Zhang, H.-X. Ren, and G.-P. Yang, "Linear reduction of backstepping algorithm based on nonlinear decoration for ship course-keeping control system," *Ocean Eng.*, vol. 147, pp. 1–8, Jan. 2018.
[25] Z. Zwierzewicz, "On the ship course-keeping control system design by using robust feedback linearization," *Polish Maritime Res.*, vol. 20, no. 1, pp. 70–76, Jan. 2013.
[26] T. Perez, *Ship Motion Control: Course Keeping and Roll Stabilization Using Rudder and Fins*. Berlin, Germany: Springer, 2006.
[27] T. Dlabač, M. Ćalasan, M. Krčum, and N. Marvučić, "PSO-based PID controller design for ship course keeping autopilot," *Brodogradnja, Teorija i Praksa Brodogradnje i Pomorske Tehnike*, vol. 70, no. 4, pp. 1–15, 2019.
[28] L. Morawski and J. Pomirski, "Design of the robust PID course keeping control system for ships," *Polish Maritime Res.*, vol. 9, no. 1, pp. 28–31, 2002.
[29] X. Zhang, *Concise Robust Control for Marine Ships*. Beijing, China: Science Press, 2012.
[30] Z. Zhang and X. Zhang, "Controller design for MIMO system with time delay using closed-loop gain shaping algorithm," *Int. J. Control, Autom. Syst.*, vol. 17, no. 6, pp. 1454–1461, May 2019.
[31] G. Zhang, X. Zhang, and W. Guan, "Stability analysis and design of integrating unstable delay processes using the mirror-mapping technique," *J. Process Control*, vol. 24, no. 7, pp. 1038–1045, Jul. 2014.
[32] Q. K. Xiao, "Ship fuzzy track keeping controller system design and simulation," M.S. thesis, Navigat. College, Dalian Maritime Univ., Dalian, China, 2015.
[33] X. Li and B.-J. Choi, "Design of obstacle avoidance system for mobile robot using fuzzy logic systems," *Int. J. Smart Home*, vol. 7, no. 3, pp. 321–328, 2013.
[34] F. Ding and Z. Yan, "Track-keeping method based on fuzzy self-tuning PID cascade control," *Ship Eng.*, vol. 31, no. 1, pp. 35–37, 2009.
[35] Z. Yan, X. Zhang, H. Zhu, and Z. Li, "Course-keeping control for ships with nonlinear feedback and zero-order holder component," *Ocean Eng.*, vol. 209, Aug. 2020, Art. no. 107461.
[36] Y. Fan, D. Mu, X. Zhang, G. Wang, and G. Chen, "Course keeping control based on integrated nonlinear feedback for a USV with pod-like propulsion," *J. Navig.*, vol. 71, no. 4, pp. 1–21, Jul. 2018.
[37] X.-K. Zhang and G.-Q. Zhang, "Design of ship course-keeping autopilot using a sine function-based nonlinear feedback technique," *J. Navigat.*, vol. 69, no. 2, pp. 246–256, Mar. 2016.
[38] B. Min, X. Zhang, and Q. Wang, "Energy saving of course keeping for ships using CGSA and nonlinear decoration," *IEEE Access*, vol. 8, pp. 141622–141631, 2020.
[39] Z. Su, X. Zhang, and X. Han, "Multitechnique concise robust control for the insulation containment space pressure control of LNG carrier," *Math. Problems Eng.*, vol. 2020, pp. 1–8, Feb. 2020.
[40] X. Jia and Y. Yang, *Ship Motion Mathematic Model*. Dalian, China: Dalian Maritime Univ. Press, 1999.
[41] C. G. Kallstrom, "Identification and adaptive control applied to ship steering," Ph.D. dissertation, Dept. Autom. Control, Lund Inst. Technol., Lund, Sweden, 1982.
[42] T. I. Fossen, K. Y. Pettersen, and R. Galeazzi, "Line-of-sight path following for dubins paths with adaptive sideslip compensation of drift forces," *IEEE Trans. Control Syst. Technol.*, vol. 23, no. 2, pp. 820–827, Mar. 2015.
[43] E. Fredriksen and K. Y. Pettersen, "Global κ-exponential way-point maneuvering of ships: Theory and experiments," *Automatica*, vol. 42, no. 4, pp. 677–687, Apr. 2006.
[44] Q. Zhang, X.-K. Zhang, and N.-K. Im, "Ship nonlinear-feedback course keeping algorithm based on MMG model driven by bipolar sigmoid function for berthing," *Int. J. Nav. Archit. Ocean Eng.*, vol. 9, no. 5, pp. 525–536, Sep. 2017.

ZUOJING SU received the B.S. and M.S. degrees from Dalian Maritime University, Dalian, China, in 2009 and 2011, respectively and became a Ph.D. candidate in Dalian Maritime University, in 2018. From September 2014 to September 2015, he was with the Faculty of Engineering and Applied Science, Memorial University of Newfoundland, St. John's, NL, Canada, as a Visiting Scholar. He is currently a Lecturer with the Navigation College, Dalian Maritime University. His research interests include ship chaotic motion and ship motion control.

XIANKU ZHANG received the Ph.D. degree from Dalian Maritime University (DMU), Dalian, China, in 1998. He is currently a Professor with DMU. He has published 19 books, of which 15 books are written as the first author, such as *Concise Robust Control for Ships* (Science Press), *Control System Modeling and Digital Simulation* (Second Edition), and *Ship Motion Control* (National Defense Industry Press). He has published more than 300 articles, of which more than 60 articles were indexed by SCI. His books and articles were totally cited more than 3000 times. His research interests include ship motion control and nonlinear feedback control.